Inorg. Chem. **2006**, *45*, 6497−6507

Systematic Study on the Structures and Reactivity of Hydrazobenzenes and Azobenzenes Bearing a Chalcogenophosphoryl Group

Masaki Yamamura, Naokazu Kano, and Takayuki Kawashima*

Department of Chemistry, Graduate School of Science, The University of Tokyo, 7-3-1 Hongo, Bunkyo-ku, Tokyo 113-0033, Japan

Received January 31, 2006

Hydrazobenzenes **3**–**5** bearing a chalcogenophosphoryl group were synthesized by palladium-catalyzed cross-coupling reactions. Their X-ray crystallographic analyses and NMR and IR spectra showed the presence of intramolecular hydrogen bonds between the N–H protons and the chalcogenophosphoryl groups. The intermolecular hydrogen bonds in phosphine oxide **3** and selenide **5** were observed in the solid state. Phosphine oxide **3**, sulfide **4**, and selenide **5** constructed a dimeric structure, a discrete monomeric structure, and a chain structure, respectively. As the chalcogen atom changed, the crystalline structures of the 2-chalcogenophosphorylhydrazobenzenes also changed. The hydrogen bonds affected the oxidation reactions of the hydrazobenzenes, and oxidation of hydrazobenzenes bearing a lighter chalcogen atom was more difficult. For azobenzenes bearing a chalcogenophosphoryl group, X-ray crystallographic analyses and NMR spectra showed little interaction between the azo group and the chalcogenophosphoryl groups. However, in the UV–vis spectra, the red shifts of the absorption maxima due to the $n \rightarrow \pi^*$ transitions indicated intramolecular interactions in the excited state, in contrast to the corresponding 4-substituted azobenzenes. In addition, photoirradiation of phosphine oxide (*E*)-**7** gave (*Z*)-**7**, whereas that of phosphine sulfide (*E*)-**8** and phosphine selenide (*E*)-**9** did not give (*Z*)-**8** and (*Z*)-**9**, suggesting that heavy chalcogen atoms quench excited states by through-space interactions. Introduction of a chalcogenophosphoryl group at the 2-position had a significant effect on the structure, spectral properties, and reactivity of hydrazobenzenes and azobenzenes. Although azobenzene (*E*)-**10** bearing a hydroxyphosphoryl group at the 2-position did not show hydrogen bonding in the crystalline state, its optical properties and photoisomerization ratio were different from those of (*E*)-**7**.

Introduction

Hydrazo compounds have both N−H bonds as well as lone pairs at nitrogen, and one of the most noteworthy reactions of hydrazo compounds is an oxidation reaction that converts a 1,2-disubstituted hydrazine group to the corresponding azo group.[1] The oxidation of hydrazobenzenes is an important method for the synthesis of azobenzenes, which have long attracted considerable interest because of their utility in dyes and optical switches.[2] Hydrazo compounds have been known to form intramolecular and/or intermolecular hydrogen bonds,[3] which must have a significant effect on their reactivity, because deprotonation plays an important role in many oxidation reactions.[4] If a hydrazobenzene bears a functional group at the 2-position that can form a hydrogen bond with the hydrazine moiety, the oxidation reaction requires more severe conditions because of the difficulty of removing a proton that is also involved with an intramolecular hydrogen bond. However, there has been little examination given to hydrazobenzenes with intramolecular hydrogen bonds.

Chalcogenophosphoryl groups, which feature a polarized P^+-Ch^- (Ch = O, S) bond, can form a hydrogen bond with

* To whom correspondence should be addressed. E-mail: takayuki@chem.s.u-tokyo.ac.jp.

(1) (a) Newbold, B. T. In *The Chemistry of the Hydrazo, Azo and Azoxy Groups Part 1*; Patai, S., Ed.; Wiley: New York, 1977; Chapter 14, pp 541−597. (b) Oxidation with H_2O_2: Cohen, S. G.; Wang, C. H. *J. Am. Chem. Soc.* **1955**, *77*, 2457−2460. (c) Oxidation with bromine: Kenner, G. W.; Stedman, R. J. *J. Chem. Soc.* **1952**, 2089−2094. (d) Oxidation with NaOCl: Burdon, J.; Morton, C. J.; Thomas, D. F. *J. Chem. Soc.* **1967**, 2621−2627.

(2) (a) Hartley, G. S. *Nature* **1937**, *140*, 281. (b) Griffiths, J. *Chem. Soc. Rev.* **1972**, 481−493. (c) Feringa, B. L. *Molecular Switches*; Wiley-VCH: Weinheim, Germany, 2001.

(3) Krueger, P. J. In *The Chemistry of the Hydrazo, Azo and Azoxy Groups Part 1*; Patai, S., Ed.; Wiley: New York, 1977; Chapter 17, pp 153−224.

(4) Newbold, B. T.; Tong, D. Y. *Can. J. Chem.* **1964**, *42*, 836−842.

10.1021/ic0601790 CCC: $33.50
Published on Web 07/01/2006

Scheme 1. Synthesis of Phosphine **2** and Phosphine Chalcogenides **3**−**5** Bearing a Hydrazobenzene Moiety

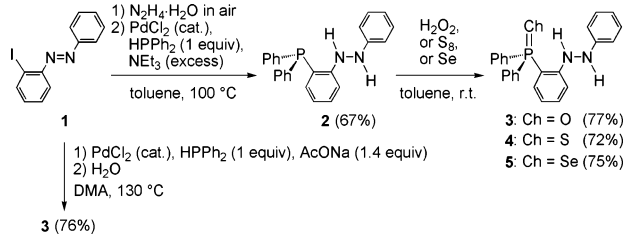

a hydrogen near the chalcogen atom, whereas less-polarized chalcogen-containing functional groups, such as sulfide (R_2S) and selenide (R_2Se), have weaker interactions with activated hydrogen atoms. One of the particular features of hydrogen bonds in phosphine chalcogenides is that the bond lengths and angles of the hydrogen bonds depend on the chalcogen atoms (O, S, and Se).[5] Therefore, compounds bearing both a hydrazine and a phosphine chalcogenide moiety are expected to construct intramolecular and/or intermolecular hydrogen bonds whose conformations and reactivities are affected by the chalcogen atoms.

We report here the synthesis, structures, and oxidation reactions of hydrazobenzenes bearing a chalcogenophosphoryl group at the 2-position and the effect of a hydrogen bond on their reactivity. We previously reported the synthesis of phosphine sulfides bearing an azobenzene moiety in our series of studies on the properties of azobenzenes bearing heteroatoms such as boron,[6] silicon,[7] and phosphorus[8] at the 2-position, which feature through-space interaction between the azo group and the heteroatoms. We also report here the structure, reactivity, and photoisomerization of azobenzenes bearing a chalcogenophosphoryl group.

Results and Discussion

Reduction of 2-iodoazobenzene **1**[9] with hydrazine monohydrate[10] in ethanol and successive cross-coupling[11] of the hydrazine intermediate with diphenylphosphine (1 equiv) using a catalytic palladium complex in toluene gave diphenyl[2-(2-phenylhydrazino)phenyl]phosphine **2** (67%) (Scheme 1). Treatment of **2**, which was prepared in situ from **1**, with hydrogen peroxide, elemental sulfur, and elemental selenium gave the corresponding phosphine chalcogenides **3** (77%), **4** (72%), and **5** (75%), respectively. Phosphine oxide **3** was also synthesized by the palladium-catalyzed cross-coupling reaction of **1** with diphenylphosphine and successive hydrolysis of the intermediary 2-diphenylphosphinoazobenzene ((*E*)-**6**) in 76% over the two steps.[8]

The structures of phosphine **2** and phosphine chalcogenides **3**−**5** were determined by X-ray crystallographic analyses. There are four and two independent molecules in the unit cell of crystals of **3** and **5**, respectively. Crystallographic data are summarized in Table 1. Selected bond lengths, bond angles, and torsion angles are shown in Table 2. ORTEP drawings of **2**−**5** are shown in Figures 1−4, respectively. The N1−N2 bond lengths of **2**−**5** fall within the range of previously observed N−N single-bond lengths.[12] The C−N−N−C torsion angles of **2** and **4** are smaller than a right angle (C6−N1−N2−C7 torsion angles: **2**, 85.02(16)°; **4**, 79.4(3)°), whereas that of the hydrazine moiety of unsubstituted hydrazobenzene (125.2°) is an obtuse angle exhibiting an anti conformation.[12] The two benzene rings of the four independent molecules of **3** are arranged in an anti conformation (C−N−N−C torsion angles: 138.5(2)−142.2(2)°). The two independent molecules of **5** show different torsion angles from each other (C−N−N−C torsion angles: 74.3(3) and 127.3(2)°).

The intramolecular distances between the oxygen and the nearest hydrogen atoms (2.09−2.16 Å) of **3** are much shorter than the sum of their van der Waals radii (2.72 Å), indicating intramolecular hydrogen bonds (Figure 2). Intermolecular distances between the oxygen and the hydrogen atoms (1.96−2.10 Å) are also short enough for hydrogen bonding. Two molecules of **3** form a dimeric structure through the intermolecular hydrogen bonds in the crystalline state. In the crystal structure of hydroxymethyldiphenylphosphine oxide, a similar dimeric structure is constituted by only intermolecular hydrogen bonds without any intramolecular hydrogen bonds (Chart 1).[5] The P═O bond lengths of **3** (1.4940(16)−1.4997(16) Å) are similar to that of triphenylphosphine oxide that coordinates intermolecularly to a hydrogen (1.495 Å)[13a] or potassium ion (1.495 Å).[13b]

In phosphine sulfide **4**, the intramolecular distance between the S1 and H1 atoms (2.47(3) Å) is sufficiently short but **4** is a discrete monomer in the crystalline state (Figure 3), in contrast to hydroxymethyldiphenylphosphine sulfide (Chart 1).[5] In phosphine selenide **5**, both the intramolecular and intermolecular distances between selenium and hydrogen (2.57(3)−2.86(3) Å) are short enough for hydrogen bonding, and **5** constructs a chain structure through the hydrogen bonds in the crystalline state (Figure 4). The bond angles of P−Ch···H (**3**: P1−O1···H5, 87.1(6)°; **4**: P1−S1···H5, 73.1(7)°) are not too wide for hydrogen bonding because of π-coordination from the chalcogen atom.[14]

In the ^{1}H NMR spectra of all the phosphine chalcogenides in solution, the N−H protons were observed in both a low-field region (**3**, $\delta_H = 8.45$; **4**, $\delta_H = 8.24$; **5**, $\delta_H = 8.26$) and

(5) Goodwin, N. J.; Henderson, W.; Nicholson, B. K. *Inorg. Chim. Acta* **2002**, *335*, 113−118.
(6) Kano, N.; Yoshino, J.; Kawashima, T. *Org. Lett.* **2005**, *7*, 3909−3911.
(7) (a) Kano, N.; Komatsu, F.; Kawashima, T. *J. Am. Chem. Soc.* **2001**, *123*, 10778−10779. (b) Kano, N.; Yamamura, M.; Komatsu, F.; Kawashima, T. *J. Organomet. Chem.* **2003**, *686*, 192−197. (c) Kano, N.; Yamamura, M.; Kawashima, T. *J. Am. Chem. Soc.* **2004**, *126*, 6250−6251.
(8) Yamamura, M.; Kano, N.; Kawashima, T. *J. Am. Chem. Soc.* **2005**, *127*, 11954−11955.
(9) Badger, G. M.; Drewer, R. J.; Lewis, G. E. *Aust. J. Chem.* **1964**, *17*, 1036−1049.
(10) Zhang, C.-R.; Wang, Y.-L. *Synth. Commun.* **2003**, *33*, 4205−4208.
(11) (a) Herd, O.; Hessler, A.; Hingst, M.; Tepper, M.; Stelzer, O. *J. Organomet. Chem.* **1996**, *522*, 69−76. (b) Brauer, D. J.; Hingst, M.; Kottsieper, K. W.; Like, C.; Nickel, T.; Tepper, M.; Stelzer, O.; Sheldrick, W. S. *J. Organomet. Chem.* **2002**, *645*, 14−26.
(12) Pestana, D. C.; Power, P. P. *Inorg. Chem.* **1991**, *30*, 528−533.
(13) For X-ray crystal structures of triphenylphosphine oxide that coordinates to proton or metals, see: (a) Llamas-Saiz, A. L.; Foces-Foces, C.; Elguero, J.; Molina, P.; Alajarín, M.; Vidal, A. *J. Chem. Soc., Chem. Commun.* **1991**, 1694−1695. (b) Crushin, V. V.; Bensimon, C.; Alper, H. *Inorg. Chem.* **1993**, *32*, 345−346.
(14) Gilheany, D. G. *Chem. Rev.* **1994**, *94*, 1339−1374.

Table 1. Crystallographic Data for **2**−**5**

	2	**3**	**4**	**5**
empirical formula	$C_{24}H_{21}N_2P$	$C_{24}H_{21}N_2OP$	$C_{24}H_{21}N_2PS$	$C_{24}H_{21}N_2PSe$
fw	368.40	384.40	400.46	447.36
T (K)	120(2)	120(2)	120(2)	120(2)
cryst syst	monoclinic	monoclinic	monoclinic	monoclinic
space group	$C2/c$	Cc	$P2_1/c$	$P2_1/n$
a (Å)	30.598(16)	41.913(17)	11.418(5)	10.570(3)
b (Å)	7.779(3)	9.860(3)	7.589(3)	25.130(7)
c (Å)	22.260(11)	19.628(8)	23.392(10)	15.553(4)
α (deg)	90	90	90	90
β (deg)	133.846(5)	102.9131(18)	90.4546(16)	94.1640(14)
γ (deg)	90	90	90	90
V (Å^3)	3821(3)	7906(5)	2027.0(14)	4120(2)
Z	8	16	4	8
ρ_{calcd} (g cm^{-3})	1.281	1.292	1.312	1.442
μ (cm^{-1})	1.55	1.56	2.51	19.12
cryst size (mm^3)	0.45 × 0.35 × 0.15	0.6 × 0.25 × 0.2	0.4 × 0.25 × 0.25	0.2 × 0.2 × 0.2
θ limit (deg)	3.30−25.00	3.09−25.00	3.20−25.00	3.09−25.00
no. of reflns collected	11 479	24 718	10 989	26 049
no. of independent reflns	3357	11622	3380	7220
params	309	1041	261	521
GOF on F^2	0.974	1.068	1.056	1.075
R1 ($I > 2\sigma(I)$)	0.0322	0.0311	0.0446	0.0297
wR2 (all data)	0.0765	0.0699	0.1326	0.0754
max peak; min hole (e Å^{-3})	0.340; −0.288	0.201; −0.214	0.574; −0.343	0.558; −0.309

Table 2. Selected Bond Lengths (Å), Bond Angles (deg), and Torsion Angles (deg) of **2**−**5**

		2	
P1−C1	1.8319(16)	C1−P1−C13	101.76(8)
P1−C13	1.8360(16)	C1−P1−C19	101.63(7)
P1−C19	1.8303(16)	C13−P1−C19	102.67(8)
N1−N2	1.4071(17)	C6−N1−N2−C7	85.02(16)
		3	
P1−O1	1.4997(16)	C1−P1−C13	106.06(10)
P1−C1	1.797(2)	C1−P1−C19	109.91(10)
P1−C13	1.800(2)	C13−P1−C19	107.36(10)
P1−C19	1.798(2)	O1−P1−C1	112.13(9)
N1−N2	1.407(3)	O1−P1−C13	110.76(10)
O1···H5	2.16(2)	O1−P1−C19	110.42(10)
O1···H27*	2.09(3)	C6−N1−N2−C7	138.5(2)
		4	
P1−S1	1.9620(10)	C1−P1−C13	105.07(11)
P1−C1	1.806(2)	C1−P1−C19	106.36(12)
P1−C13	1.818(2)	C13−P1−C19	106.14(11)
P1−C19	1.807(2)	S1−P1−C1	114.83(8)
N1−N2	1.400(3)	S1−P1−C13	112.34(9)
S1···H5	2.47(3)	S1−P1−C19	111.47(8)
S1···H6′	3.59(3)	C6−N1−N2−C7	79.4(3)
		5	
P1−Se1	2.1256(7)	C1−P1−C13	105.32(9)
P1−C1	1.808(2)	C1−P1−C19	106.34(10)
P1−C13	1.816(2)	C13−P1−C19	104.61(9)
P1−C19	1.808(2)	Se1−P1−C1	112.64(7)
N1−N2	1.384(3)	Se1−P1−C13	114.77(7)
Se1···H5	2.69(3)	Se1−P1−C19	112.40(7)
Se1···H27	2.71(3)	C6−N1−N2−C7	74.3(3)
Se2···H26	2.57(3)	C30−N3−N4−C31	127.3(2)
Se2···H6*	2.86(3)		

almost the same region (**3**, $\delta_H = 5.62$; **4**, $\delta_H = 5.55$; 5, $\delta_H = 5.57$) as that of unsubstituted hydrazobenzene ($\delta_H = 5.62$).[15] The low-field shifts of the N−H proton indicate interaction between the N−H protons and the chalcogenophosphoryl groups in solution. In contrast, the N−H proton of phosphine **2** was not observed in a lower field (**2**, $\delta_H = 5.60$, 6.43) than those of phosphine chalcogenides **3**−**5**, which is due to a weak interaction between the lone pair on

(15) Spectral data of unsubstituted hydrazobenzene were measured under the same conditions as those of the other compounds.

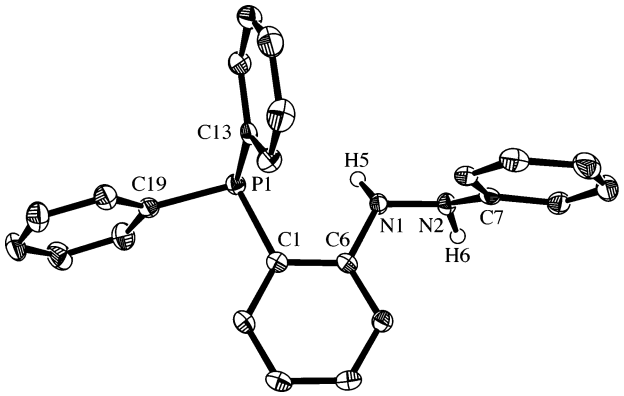

Figure 1. ORTEP drawing with the thermal ellipsoid plot (50% probability level) of **2**. Hydrogen atoms attached to the benzene rings were omitted for clarity.

phosphine and the N−H proton.[16] In the ^{31}P NMR spectra, the chemical shifts of **2**−**5** (**2**, $\delta_P = -21.9$; **3**, $\delta_P = 36.1$; **4**, $\delta_P = 39.4$; **5**, $\delta_P = 26.4$) were very different from those of triphenylphosphine ($\delta_P = -5.8$), triphenylphosphine oxide ($\delta_P = 30.9$), sulfide ($\delta_P = 42.6$), and selenide ($\delta_P = 35.7$) but similar to those of (2-aminophenyl)diphenylphosphine ($\delta_P = -20.8$), its oxide ($\delta_P = 35.9$), sulfide ($\delta_P = 39.0$), and selenide ($\delta_P = 27.4$), respectively, which results from the hydrogen bond and the electron-donating effect of the 2-phenylhydrazino group at the ortho position of the phosphorus substituents.[17] Phosphine oxide **3** showed a low-field shift by 5.0 ppm relative to triphenylphosphine oxide because of the hydrogen bond. Phosphine selenide **5** showed a doublet (δ_{Se} −260.2) with a coupling constant ($^1J_{(Se,P)} = 683.2$ Hz) between those of $Ph_3PSeAlCl_3$ ($\delta_{Se} = -190$, $^1J_{(Se,P)} = 540$ Hz) and Ph_3PSe ($\delta_{Se} = -275$, $^1J_{(Se,P)} = 736$ Hz).[18]

(16) Külh, O.; Lönnecke, P. *Inorg. Chem.* **2002**, *42*, 4315−4317.
(17) (a) Copper, M. K.; Downes, J. M.; Duckworth, P. A.; Tiekink, E. R. T. *Aust. J. Chem.* **1992**, *45*, 595−609. (b) Ainscough, E. W.; Brodie, A. M.; Burrell, A. K.; Fan, X.; Halstead, M. J. R.; Kennedy, S. M. F.; Waters, J. M. *Polyhedron* **2000**, *19*, 2585−2592.

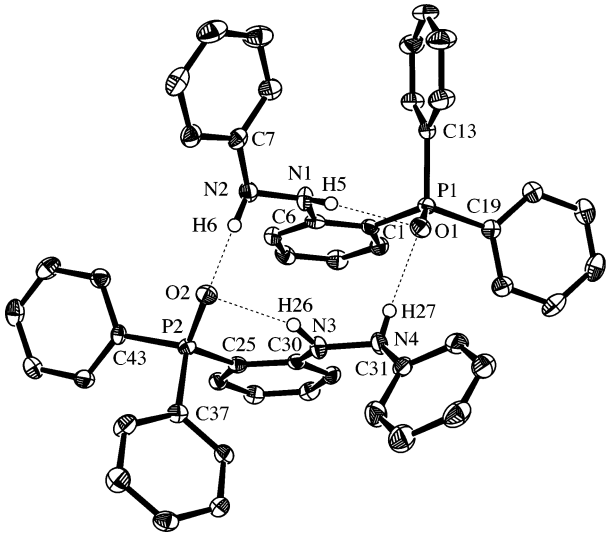

Figure 2. ORTEP drawing with the thermal ellipsoid plot (50% probability level) of a dimeric structure composed of two of four independent molecules of **3** through intermolecular hydrogen bonds. Hydrogen atoms attached to the benzene rings were omitted for clarity.

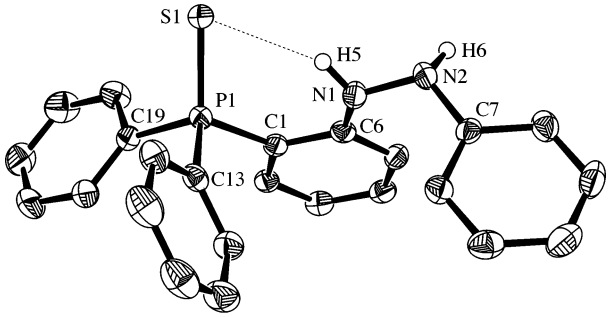

Figure 3. ORTEP drawing with the thermal ellipsoid plot (50% probability level) of **4**. Hydrogen atoms attached to the benzene rings were omitted for clarity.

The IR spectra also suggest the presence of hydrogen bonds in **3**−**5**. In CCl_4 solution, compounds **3**−**5** showed two absorption bands due to N−H stretching. The absorption bands in higher frequencies (**3**, 3392 cm^{-1}; **4**, 3383 cm^{-1}; **5**, 3382 cm^{-1}), which were observed in almost the same region as that of unsubstituted hydrazobenzene (3389 cm^{-1}),[15] are assigned to N−H stretching without a hydrogen bond. The other absorption bands (**3**, 3269 cm^{-1}; **4**, 3244 cm^{-1}; **5**, 3213 cm^{-1}) of N−H stretching in **3**−**5** were shifted to lower frequencies than those of unsubstituted hydrazobenzene, upon chalcogen atoms of phosphine chalcogenides going down the periodic table.[19] In the solid state, the shifts to lower frequencies were also observed for **3**−**5**. Phosphine oxide **3** and phosphine selenide **5** showed two N−H absorption bands (**3**, 3279 and 3231 cm^{-1}; **5**, 3289 and 3221 cm^{-1}), both of which were observed at lower frequency than that of hydrazobenzene (3329 cm^{-1}),[15] suggesting that the hydrogen atoms interact with oxygen or selenium atoms through intermolecular and intramolecular hydrogen bonds. In phosphine sulfide **4**, one of the two absorption bands was observed at much lower frequency (3244 cm^{-1}), and the other one (3311 cm^{-1}) was not significantly different from that of unsubstituted hydrazobenzene. These shifts to lower frequencies in the IR spectra in the solid state are consistent with the crystal structures revealed by the X-ray crystallographic analyses.

Oxidation of hydrazobenzenes **3**−**5** with an excess of bromine gave azobenzene (*E*)-**7** quantitatively (Scheme 2 and Table 3, entries 1−3). Upon the use of pyridinium tribromide (1 equiv), oxidation of **3**−**5** gave the corresponding azobenzenes (*E*)-**7** (100%), (*E*)-**8** (89%), and (*E*)-**9** (26%), respectively (entries 4−6). These results indicate that although bromine oxidizes the hydrazine, oxidation of the chalcogen moiety takes place competitively. Whereas hydrazobenzene **3** bearing a phosphine oxide moiety was not oxidized by *t*-BuOCl at all (entry 7), phosphine sulfide **4** and selenide **5** were oxidized under the same conditions. Similarly to bromine, 1 equiv of *t*-BuOCl oxidized **4** and **5** to give (*E*)-**8** (61%) and (*E*)-**9** (45%), respectively, whereas an excess of the oxidant gave only (*E*)-**7** (entries 8−11). When hydrogen peroxide was used as the oxidant, only **5** was oxidized among **3**−**5** (entries 12−15). The reaction of **5** with 1 equiv of hydrogen peroxide gave (*E*)-**9** (28%), whereas an excess of hydrogen peroxide gave (*E*)-**7** (40%) together with **3** (60%). Compound **3** was formed by oxidation of the selenium in **5** before the oxidation of the hydrazine moiety. The oxidation reaction proceeds more easily upon the chalcogen of the phosphine chalcogenides going down the periodic table. This order is consistent with the order of the oxidation potential of phosphine chalcogenide moieties, which can affect the oxidation potential of the hydrazine moiety through the intramolecular interaction. The oxidation reactions of various hydrazobenzenes depend on the substituents in many cases. Electron-withdrawing groups and bulky groups at the 2-position of hydrazobenzene make oxidation difficult.[4] However, the reactivity of the hydrazobenzenes in oxidation depends on both the strength of the hydrogen bond and the oxidation potential of the chalcogen moiety, considering the change in reactivity by the chalcogen atoms.

Hydrazobenzene **2** bearing a diphenylphosphino group without an intramolecular hydrogen bond was similarly oxidized. When phosphine **2** was treated with 1 equiv of *t*-BuOCl, many signals were observed in the ^{31}P NMR spectrum. Oxidation of **2** with an excess amount of *t*-BuOCl gave (*E*)-**7** quantitatively (Scheme 3).

Treatment of (*E*)-**7** with trimethylsilyl triflate and successive hydrolysis gave hydroxyphosphonium salt (*E*)-**10**. The formation mechanism of (*E*)-**7** from **2** is most likely explained by conversion of the phosphine moiety of **2** to a chlorophosphonium salt **11**, successive oxidation of the hydrazine moiety to an azo group, and hydrolysis of the phosphonium salt (*E*)-**12** (Scheme 4). If the hydrazine moiety of **2** was oxidized before the phosphine moiety, intermediary 2-phosphinoazobenzene (*E*)-**6** would have been hydrolyzed to **3** in the manner reported previously.[8]

Azobenzenes (*E*)-**15**−(*E*)-**17** bearing a chalcogenophosphoryl group at the 4-position were synthesized by the reactions of 4-phosphinoazobenzene (*E*)-**14**, which was obtained by treatment of 4-iodoazobenzene **13** with butyl-

(18) Burford, N. *Coord. Chem. Rev.* **1992**, *112*, 1−18.
(19) Zhang, Q.; Aucott, S. M.; Slawin, A. M. Z.; Woollins, J. D. *Eur. J. Inorg. Chem.* **2002**, 1635−1646.

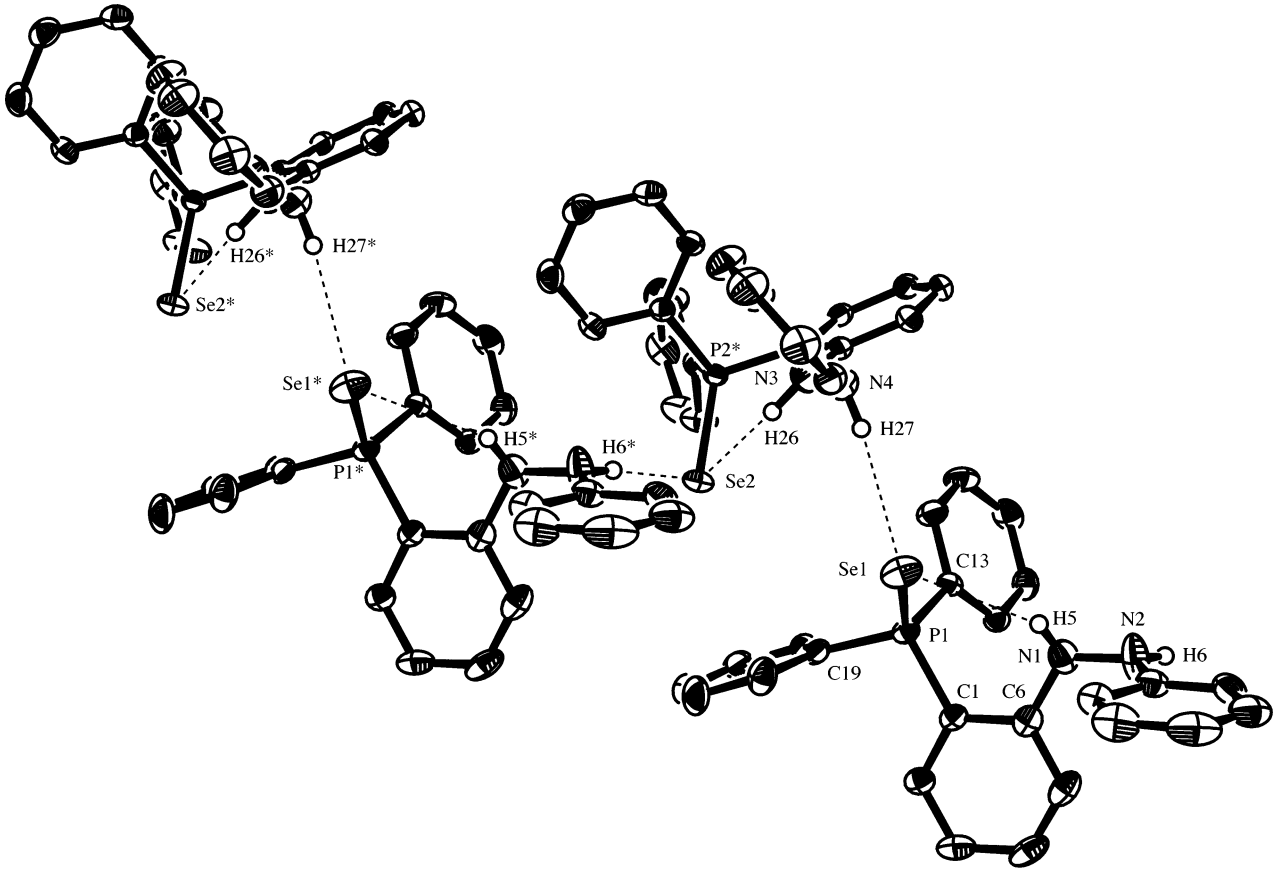

Figure 4. ORTEP drawing with the thermal ellipsoid plot (50% probability level) of part of a chain structure composed of **5** through intermolecular hydrogen bonds. Hydrogen atoms attached to the benzene rings were omitted for clarity.

Chart 1. Intermolecular Hydrogen Bonds of Hydroxymethyldiphenylphosphine Oxide, Sulfide, and Selenide

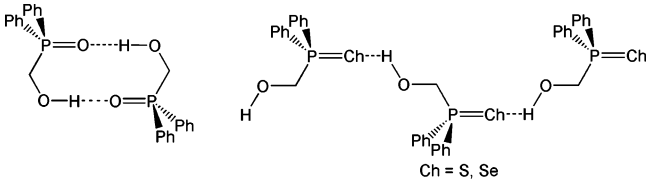

Scheme 2. Oxidation Reactions of Hydrazobenzenes **3**−**5**

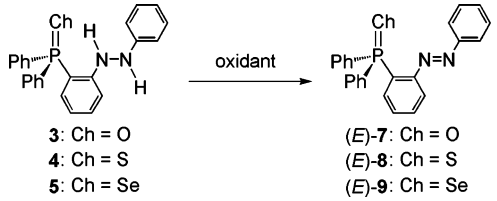

lithium and chlorodiphenylphosphine (Scheme 5) with hydrogen peroxide, elemental sulfur, and elemental selenium, respectively, in good yields.

The structures of azobenzenes (*E*)-**7**−(*E*)-**10** were determined by X-ray crystallographic analyses. ORTEP drawings of (*E*)-**7**−(*E*)-**10** are shown in Figures 5 and 6. Crystallographic data are summarized in Table 4. Selected bond lengths and angles are shown in Table 5. The N═N bond lengths are almost the same as that of unsubstituted azobenzene.[20] The bond angles around the phosphorus atom are slightly different from those of the corresponding triphenylphosphine chalcogenides, $Ph_3P{=}Ch$.[21] The long distances between the nitrogen atom and the chalcogen atom indicate little interaction between the azo group and the chalcogenophosphoryl groups in the crystalline states. Com-

(20) Bouwstra, J. A.; Schouten, A.; Kroon, J. *Acta Crystallogr., Sect. C* **1983**, *39*, 1121−1123.

Table 3. Oxidation of Hydrazobenzenes **3**−**5** with Some Oxidants

entry	substrate	oxidant	product	yield (%)
1	**3**	Br_2 (excess)	(*E*)-**7**	quant.[a]
2	**4**	Br_2 (excess)	(*E*)-**7**	quant.[a]
3	**5**	Br_2 (excess)	(*E*)-**7**	quant.[a]
4	**3**	py·$H^+Br_3^-$ (1 equiv)	(*E*)-**7**	100[b]
5	**4**	py·$H^+Br_3^-$ (1 equiv)	(*E*)-**8**	89[b]
6	**5**	py·$H^+Br_3^-$ (1 equiv)	(*E*)-**9**	26[b]
7	**3**	*t*-BuOCl (excess)	no reaction	
8	**4**	*t*-BuOCl (excess)	(*E*)-**7**	quant.[a]
9	**5**	*t*-BuOCl (excess)	(*E*)-**7**	quant.[a]
10	**4**	*t*-BuOCl (1 equiv)	(*E*)-**8**	61[b]
11	**5**	*t*-BuOCl (1 equiv)	(*E*)-**9**	45[b]
12	**3**	H_2O_2 (excess)	no reaction	
13	**4**	H_2O_2 (excess)	no reaction	
14	**5**	H_2O_2 (excess)	(*E*)-**7**	40[a,c]
15	**5**	H_2O_2 (1 equiv)	(*E*)-**9**	28[b]

[a] Quantitative; the yields were confirmed by ^1H and ^{31}P NMR spectra. [b] Isolated yields. [c] Compound **3** was obtained in 60% yield as a byproduct.

Scheme 3. Synthesis and Photoisomerization of Hydroxyphosphonium Salt (*E*)-**10**

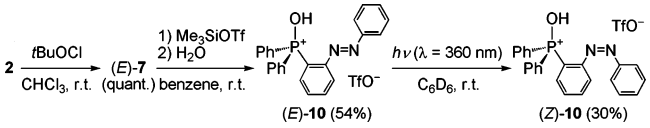

Scheme 4. Reaction Mechanism of the Oxidation of Phosphine **2**

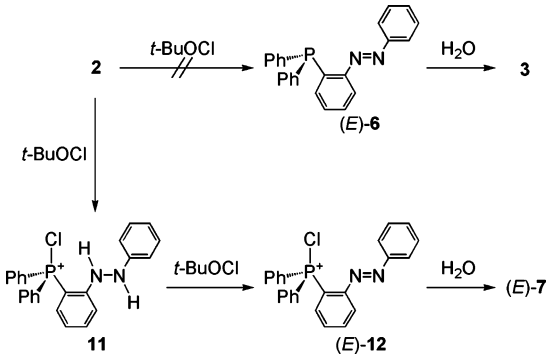

Scheme 5. Synthesis of Azobenzenes Bearing a Chalcogenophosphoryl Group at the 4-Position

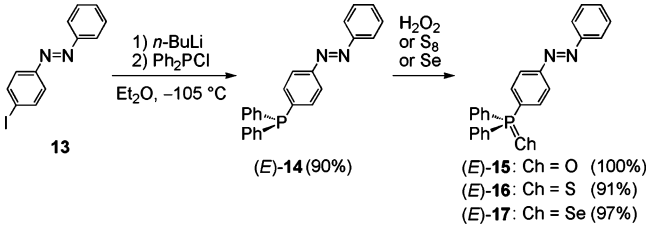

pound (*E*)-**10** may have a hydrogen bond between the hydrogen atom of the hydroxy group and the azo group. However, the crystal structure of (*E*)-**10** revealed that the P−O bond length of (*E*)-**10** (1.5474(16) Å) and the bond angles around the phosphorus are similar to those of hydroxytriphenylphosphonium salts (1.550 Å).[22] The hydrogen atom of the O−H group was not located between the oxygen and nitrogen atoms, suggesting that there is no hydrogen bond between the hydroxyphosphonium moiety and the azo group.

In the ^{31}P NMR spectra, azobenzenes (*E*)-**7**−(*E*)-**9** showed chemical shifts similar to the corresponding triphenylphosphine chalcogenides. Judging from the ^{31}P chemical shifts, azobenzenes (*E*)-**7**−(*E*)-**9** have no intramolecular interaction between the azo group and the chalcogenophosphoryl groups in solution, in contrast to hydrazobenzenes **3**−**5**. In the UV−vis spectra, (*E*)-**15**−(*E*)-**17** showed two absorption maxima, assignable to the $\pi \rightarrow \pi^*$ transitions of the azo group (λ_{max} = 324 nm for (*E*)-**15**−(*E*)-**17**) and to the $n \rightarrow \pi^*$ transitions (λ_{max} = 440 nm for (*E*)-**15**−(*E*)-**17**). These transitions were almost the same as those of unsubstituted azobenzene (λ_{max} = 320 and 440 nm).[23] However, chloroform solutions of (*E*)-**7**−(*E*)-**9** showed that the absorption maxima assignable to the $\pi \rightarrow \pi^*$ transitions of the azo group (λ_{max} = 327 nm for (*E*)-**7**, 328 nm for (*E*)-**8**, and 325 nm for (*E*)-**9**) were almost the same as that of unsubstituted azobenzene (λ_{max} = 320 nm), whereas the absorption maxima assigned to the $n \rightarrow \pi^*$ transitions (λ_{max} = 458 nm for (*E*)-**7**, 465 nm for (*E*)-**8**, and 465 nm for (*E*)-**9**) were observed at longer wavelengths than that of unsubstituted azobenzene (λ_{max} = 440 nm), in contrast to those of (*E*)-**15**−(*E*)-**17**. The red shift is considered to be caused by the interaction between the lone pair on the nitrogen atom and the chalcogen atom in the excited state. The bulkiness of the substituent at the 2-position can make a contribution to the red shift of the $n \rightarrow \pi^*$ transitions because of repulsion between the substituent at the 2-position and the lone pair on the nitrogen.[24] However, the red shift

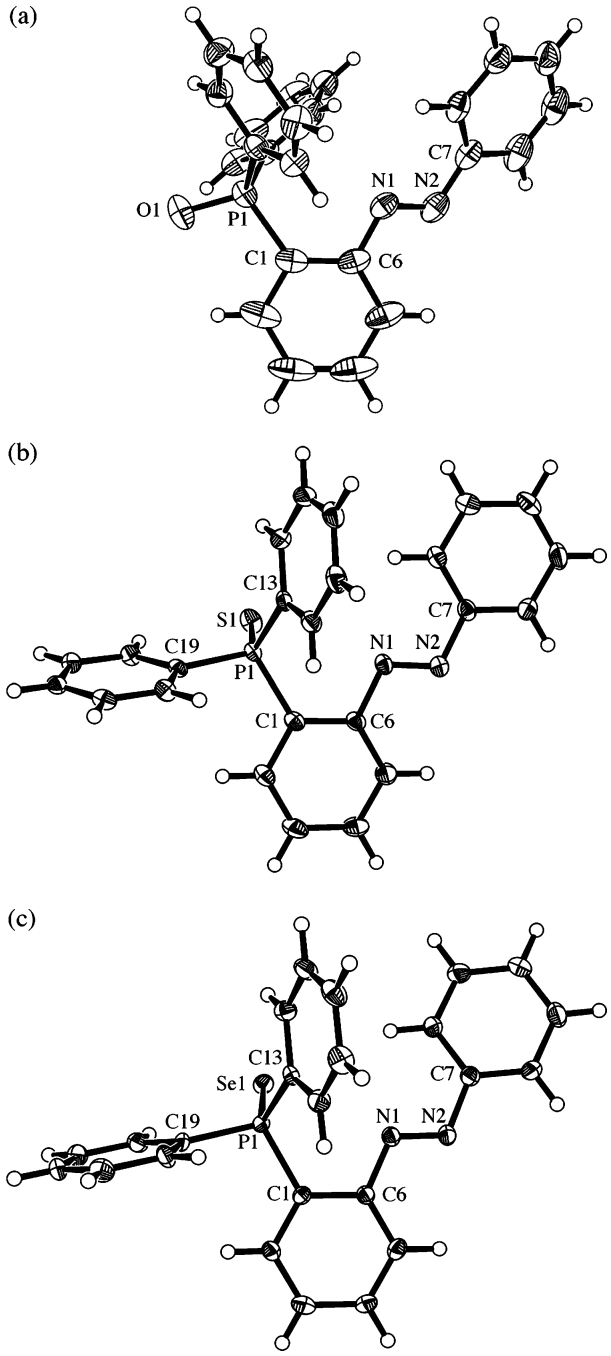

Figure 5. ORTEP drawings with the thermal ellipsoid plot (50% probability level): (a) phosphine oxide (*E*)-**7**; (b) phosphine sulfide (*E*)-**8**; (c) phosphine selenide (*E*)-**9**.

(21) For X-ray crystal structures of triphenylphosphine chalcogenides, see: (a) Thomas, J. A.; Hamor, T. A. *Acta Crystallogr., Sect. C* **1993**, *49*, 355−357. (b) Ziemer, B.; Rabis, A.; Steinberger, H.-U. *Acta Crystallogr., Sect. C* **2000**, *56*, e58−e59. (c) Codding, P. W.; Kerr, K. A. *Acta Crystallogr., Sect. B* **1979**, *35*, 1261−1263.

(22) Lane, H. P.; McAuliffe, C. A.; Pritchard, R. G. *Acta Crystallogr., Sect. C* **1992**, *48*, 2002−2004.

(23) Spectral data and the photoisomerization ratio of unsubstituted azobenzene were measured under the same conditions as those of the other compounds.

(24) Forber, C. L.; Kelusky, E. C.; Bunce, N. J.; Zerner, M. C. *J. Am. Chem. Soc.* **1985**, *107*, 5884−5890.

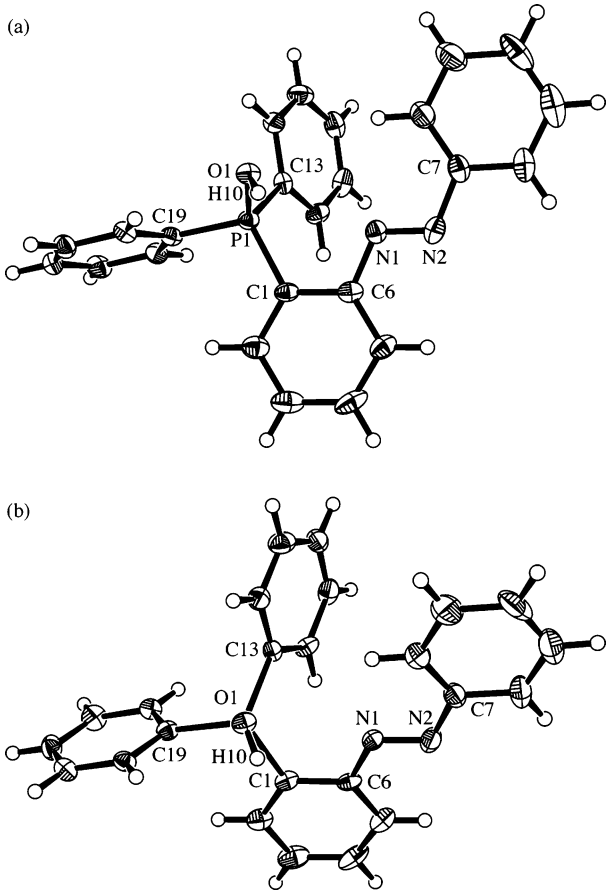

Figure 6. ORTEP drawings with the thermal ellipsoid plot (50% probability level) of (*E*)-**10**. A triflate anion was omitted for clarity. (a) Side view from the azobenzene moiety. (b) View from the direction to the O−P bond.

Table 4. Crystallographic Data for (*E*)-**7**−(*E*)-**10**

	(*E*)-**7**	(*E*)-**8**	(*E*)-**9**	(*E*)-**10**
empirical formula	$C_{24}H_{19}N_2OP$	$C_{24}H_{19}N_2PS$	$C_{24}H_{19}N_2PSe$	$C_{25}H_{20}F_3N_2O_4PS$
fw	382.38	398.44	445.34	532.46
T (K)	120(2)	120(2)	120(2)	120(2)
cryst syst	monoclinic	monoclinic	monoclinic	hexagonal
space group	$P2_1/c$	$P2_1$	$P2_1/n$	$P6_1$
a (Å)	10.079(7)	9.171(3)	8.604(4)	10.1017(5)
b (Å)	9.815(7)	14.590(5)	23.038(9)	10.1017(5)
c (Å)	20.357(14)	15.752(5)	20.764(9)	42.334(4)
α (deg)	90	90	90	90
β (deg)	97.234(3)	101.1255(16)	91.7375(15)	90
γ (deg)	90	90	90	120
V (Å^3)	1998(2)	2068.1(12)	4114(3)	3741.2(4)
Z	4	4	8	6
ρ_{calcd} (g cm^{-3})	1.271	1.280	1.438	1.418
μ (cm^{-1})	1.54	2.45	19.15	2.51
cryst size (mm^3)	0.2 × 0.2 × 0.2	0.5 × 0.3 × 0.25	0.2 × 0.2 × 0.2	0.35 × 0.3 × 0.2
θ limit (deg)	3.04−25.00	3.09−25.00	3.07−25.00	3.00−25.01
no. of reflns collected	10 858	13 254	25 529	16 064
no. of independent reflns	3427	7099	7208	3989
params	253	506	505	326
GOF on F^2	1.086	1.048	1.109	0.894
R1 ($I > 2\sigma(I)$)	0.0578	0.0218	0.0533	0.0314
wR2 (all data)	0.1744	0.0561	0.1519	0.0531
max peak; min hole (e Å^{-3})	1.141; −0.341	0.277; −0.150	2.220; −0.543	0.265; −0.245

was not caused by bulkiness alone, considering the absorption maxima (λ_{max} = 326 and 455 nm) of 2-(methyldiphenylsilyl)-azobenzene, whose bulkiness is almost the same as (*E*)-**7**−(*E*)-**9**.[25] Whereas (*E*)-**10** showed a small red shift in the $\pi \rightarrow \pi^*$ transition (λ_{max} = 332 nm), its $n \rightarrow \pi^*$ transition (λ_{max} = 460 nm) was almost the same as that of (*E*)-**7**. If the azo group had been protonated by the intramolecular hydroxy group, the $n \rightarrow \pi^*$ transition would have been blue-shifted. The UV−vis spectrum of (*E*)-**10** suggests that there is little interaction between the azo group and the hydroxy group of (*E*)-**10** in solution.

Table 5. Selected Bond Lengths (Å) and Angles (deg) of (*E*)-**7**−(*E*)-**10**

		(*E*)-**7**	
P1−O1	1.481(2)	C1−P1−C13	109.39(12)
P1−C1	1.827(3)	C1−P1−C19	108.42(12)
P1−C13	1.803(3)	C13−P1−C19	107.73(12)
P1−C19	1.803(3)	O1−P1−C1	109.52(13)
N1−N2	1.262(3)	O1−P1−C13	111.28(11)
		O1−P1−C19	110.44(13)
		(*E*)-**8**	
P1−S1	1.9477(7)	C1−P1−C13	107.67(7)
P1−C1	1.8200(17)	C1−P1−C19	106.67(7)
P1−C13	1.8143(15)	C13−P1−C19	103.19(7)
P1−C19	1.8265(15)	S1−P1−C1	111.91(5)
N1−N2	1.2571(17)	S1−P1−C13	114.47(5)
		S1−P1−C19	112.28(5)
		(*E*)-**9**	
P1−Se1	2.1045(13)	C1−P1−C13	107.38(18)
P1−C1	1.811(4)	C1−P1−C19	105.40(18)
P1−C13	1.813(4)	C13−P1−C19	104.50(18)
P1−C19	1.832(4)	Se1−P1−C1	112.87(13)
N1−N2	1.248(5)	Se1−P1−C13	114.58(13)
		Se1−P1−C19	111.37(13)
		(*E*)-**10**	
P1−O1	1.5474(16)	C1−P1−C13	109.18(12)
P1−C1	1.798(3)	C1−P1−C19	107.28(12)
P1−C13	1.785(3)	C13−P1−C19	109.99(12)
P1−C19	1.783(2)	O1−P1−C1	115.71(11)
N1−N2	1.261(2)	O1−P1−C13	107.45(11)
		O1−P1−C19	107.17(11)

Scheme 6. Photoisomerization of Azobenzenes (*E*)-**7**−(*E*)-**9** Bearing a Chalcogenophosphoryl Group at the 2-Position

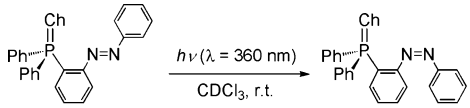

(*E*)-**7**: Ch = O
(*E*)-**8**: Ch = S
(*E*)-**9**: Ch = Se

(*Z*)-**7** (90%)
(*Z*)-**8** (0%)
(*Z*)-**9** (0%)

Photoisomerization of (*E*)-**7** was achieved by 1 h of irradiation in $CDCl_3$ with a high-pressure mercury lamp equipped with a monochromator (λ = 360 nm) to give (*Z*)-**7** (90%), and irradiation of (*Z*)-**7** through a monochromator (λ = 445 nm) gave (*E*)-**7** (81%) (Scheme 6). The ratio of photoisomerization of **7** was slightly different from that of unsubstituted azobenzene.[24] Considering that the chemical shift of (*Z*)-**7** (δ_P = 28.1) is almost the same as that of (*E*)-**7** in ^{31}P NMR spectra, (*Z*)-**7** also has little interaction between the azo group and the oxygen atom. The 4-substituted azobenzenes (*E*)-**15**−(*E*)-**17** were similarly isomerized to the corresponding (*Z*)-isomers by photoirradiation (Scheme 7).

In contrast, irradiation of (*E*)-**8** and (*E*)-**9** did not give the corresponding (*Z*)-isomers at all under the same conditions. Considering the successful photoisomerization of (*E*)-**15**−

(25) Kano, N.; Komatsu, F.; Kawashima, T. *Chem. Lett.* **2001**, 338−339.

Scheme 7. Photoisomerization of Azobenzenes (*E*)-**15**−(*E*)-**17** Bearing a Chalcogenophosphoryl Group at the 4-Position

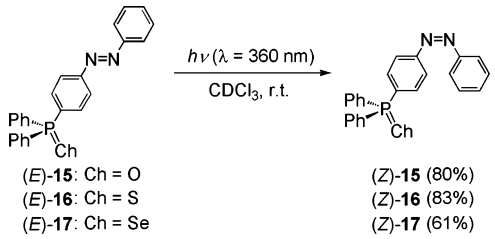

(*E*)-**17**, photoisomerization of (*E*)-**8** and (*E*)-**9** was prevented by the intramolecular through-space interaction between the azo group and the chalcogen atom. The excited states of (*E*)-**8** and (*E*)-**9** would be quenched by the heavier chalcogen atoms, sulfur and selenium, respectively, and hence were not isomerized. Low conversion in the photoisomerization was also observed in the azobenzene (*E*)-**10** bearing a hydroxy group, which can potentially coordinate to the azo group. Although photoirradiation of (*E*)-**7** caused isomerization to (*Z*)-**7** in high yield, the conversion was not efficient for (*E*)-**10** (Scheme 3). Interaction between the hydrogen atom in the hydroxy group and the azo group in solution would be one reason for the low yield of photoisomerization to (*E*)-**10**.

Conclusion

In summary, hydrazobenzenes **3**−**5** bearing a chalcogenophosphoryl group were synthesized by palladium-catalyzed cross-coupling reactions. The intramolecular hydrogen bonds between the N−H proton of the hydrazine moiety and the chalcogenophosphoryl groups in **3**−**5** were confirmed by their X-ray crystallographic analyses and NMR and IR spectra. The intermolecular hydrogen bonds in phosphine oxide **3** and selenide **5** were also observed in the solid state. These hydrogen bonds result in a dimeric structure in phosphine oxide **3**, a discrete monomeric structure in phosphine sulfide **4**, and a chain structure in phosphine selenide **5**. The different chalcogen atoms induce changes in the highly ordered structures through the hydrogen bonds between hydrazine and phosphine chalcogenide moieties, which is an interesting method for construction of a self-assembly system. The hydrogen bonds affect the oxidation reactions of the hydrazobenzenes, and the oxidation reactions of hydrazobenzenes bearing lighter chalcogen atoms are more difficult. It is interesting that not only the structures but also the reactivity of **3**−**5** are changed by the chalcogen atom. In the azobenzenes bearing a chalcogenophosphoryl group at the 2-position, the X-ray crystallographic analyses and the NMR spectra showed little interaction between the azo group and the chalcogenophosphoryl groups. However, in the UV−vis spectra, the red shifts of the absorption maxima due to the $n \rightarrow \pi^*$ transitions indicate intramolecular interactions in the excited state in contrast to the corresponding 4-substituted azobenzenes. In addition, photoirradiation of (*E*)-**8** and (*E*)-**9** did not give (*Z*)-**8** and (*Z*)-**9**, whereas that of (*E*)-**7** gave (*Z*)-**7**, suggesting that heavy chalcogen atoms quench excited states by through-space interactions. Introduction of a chalcogenophosphoryl group at the 2-position affects the optical properties and photoreactivity of the azobenzene, which can be further altered by using different chalcogen atoms. These results suggest that the structure, spectral properties, and reactivity of other compounds bearing both a phosphine chalcogenide group and a functional group that may interact with the chalcogen atom can be controlled by changing the chalcogen atom.

Experimental Session

General Procedure. Solvents were purified before use. All reactions were carried out under an argon atmosphere unless otherwise noted. Melting points were determined on a Yanaco micro melting point apparatus. The ^{1}H NMR (500 MHz), ^{13}C NMR (126 MHz),^{31}P NMR (162 MHz), and ^{77}Se NMR (95 MHz) spectra were measured at 293 K with a JEOL A500 spectrometer using $CHCl_3$ (δ_H = 7.25) and $CDCl_3$ (δ_C = 77) as internal standards and tributylphosphine ($\delta_P = -31.8$) and diphenyl diselenide ($\delta_{Se} = 480$) as external standards. The ^{19}F NMR (376 MHz) spectra were measured with a JEOL AL400 spectrometer using CF_3COOH ($\delta_F = -77$) as an external standard. Infrared spectra were recorded on a JASCO V-530. Mass spectra were recorded with a JEOL JMX-SX 102 mass spectrometer. Elemental analyses were performed by the Microanalytical Laboratory of the Department of Chemistry, Faculty of Science, The University of Tokyo. 2-Iodoazobenzene and 4-iodoazobenzene were prepared according to the literature.[9]

Synthesis of Diphenyl[2-(1-phenylhydrazino)phenyl]phosphine (2). A mixture of 2-iodoazobenzene (**1**) (1.00 g, 3.24 mmol) and hydrazine monohydrate (2 mL) in EtOH (30 mL) was stirred vigorously at 80 °C for 5 h under air conditioning. After the addition of water, extraction with $CHCl_3$ and evaporation of the solvent gave a crude solid of 2-iodohydrazobenzene. The crude solid was dissolved in toluene (20 mL), and the solution was treated with $PdCl_2$ (10 mg, 56 μmol), diphenylphosphine (0.62 mL, 3.6 mmol), and triethylamine (1 mL, 7 mmol). After the reaction solution was stirred at 100 °C for 12 h, washing with water, evaporation of the solvent, and recrystallization of the crude solid from EtOH gave a colorless solid of **2** (0.80 g, 67%). Mp: 157−158 °C. ^{1}H NMR (500 MHz, $CDCl_3$): δ 5.50 (brs, 1H), 6.43 (brs, 1H), 6.52 (d, J_{H-H} = 8.0 Hz, 2H), 6.66 (d, J_{H-H} = 8.0 Hz, 1H), 6.75 (t, J_{H-H} = 7.5 Hz, 1H), 6.77−6.80 (m, 1H), 7.06 (dd, J_{H-H} = 7.5 Hz, J_{H-P} = 5.0 Hz, 1H), 7.13 (t, J_{H-H} = 8.0 Hz, 2H), 7.20 (t, J_{H-H} = 8.0 Hz, 1H), 7.32−7.38 (m, 10H). ^{13}C{^{1}H} NMR (126 MHz, $CDCl_3$): δ 111.52 (s, *C*H), 112.27 (s, *C*H), 118.45 (d, J_{C-P} = 10.6 Hz, *C*P), 119.63 (s, *C*H), 119.84 (s, *C*H), 128.71 (d, J_{C-P} = 7.1 Hz, *C*H), 129.06 (s, *C*H), 129.26 (s, *C*H), 130.68 (s, *C*H), 133.81 (s, *C*H), 133.96 (s, *C*H), 134.96 (d, J_{C-P} = 6.9 Hz, *C*P), 148.50 (s, *C*N), 151.23 (s, *C*N). ^{31}P NMR (162 MHz, $CDCl_3$): δ −21.9 (s). HRMS (FAB) *m*/*z*: calcd for $C_{24}H_{21}N_2P$, 368.1442; found, 368.1439 [M^+].

Synthesis of Diphenyl[2-(1-phenylhydrazino)phenyl]phosphine oxide (3). To a toluene solution (20 mL) of **2**, which was prepared in situ from **1** (1.00 g, 3.24 mmol), was added 30% H_2O_2(aq) (10 mL). After the addition of water, extraction with $CHCl_3$ and evaporation of the solvent gave a crude oil. The crude oil was separated by alumina-gel chromatography (eluent: $CHCl_3$), and recrystallization from ethanol/$CHCl_3$ gave a colorless solid of **3** (0.96 g, 77%). Mp: 166−168 °C. ^{1}H NMR (500 MHz, $CDCl_3$): δ 5.62 (brs, 1H), 6.59 (d, $^3J_{H-H}$ = 8.0 Hz, 2H), 6.66 (td, $^3J_{H-H}$ = 7.5 Hz, $^4J_{H-H}$ = 1.5 Hz, 1H), 6.75 (t, $^3J_{H-H}$ = 7.5 Hz, 1H), 6.83 (ddd, $^3J_{H-P}$ = 14.5 Hz, $^3J_{H-H}$ = 7.5 Hz, $^4J_{H-H}$ = 1.5 Hz, 1H), 7.08 (t, $^3J_{H-H}$ = 8.0 Hz, 2H), 7.15 (ddd, $^3J_{H-H}$ = 7.5 Hz, J_{H-H} = 4.8 Hz, ^4J(H,H) = 1.5 Hz, 1H), 7.32 (t, $^3J_{H-H}$ = 7.5 Hz, 1H), 7.49 (td, $^3J_{H-H}$ = 8.0 Hz, J_{H-P} = 2.8 Hz, 4H), 7.59 (td, $^3J_{H-H}$ = 7.5 Hz,

$^4J_{H-H}$ = 1.5 Hz, 2H), 7.68 (ddd, $^3J_{H-P}$ = 12.0 Hz, $^3J_{H-H}$ = 7.5 Hz, $^4J_{H-H}$ = 1.5 Hz, 4H), 8.45 (brs, 1H). $^{13}C\{^1H\}$ NMR (126 MHz, $CDCl_3$): δ 111.54 (d, $^1J_{C-P}$ = 104.7 Hz, *C*P), 112.03 (d, J_{C-P} = 7.7 Hz, *C*H), 112.24 (s, *C*H), 117.39 (d, J_{C-P} = 12.6 Hz, *C*H), 119.66 (s, *C*H), 128.57 (d, J_{C-P} = 12.4 Hz, *C*H), 129.12 (s, *C*H), 132.02 (d, $^1J_{C-P}$ = 104.8 Hz, *C*P), 132.11 (s, *C*H), 132.44 (s, *C*H), 133.12 (d, J_{C-P} = 10.8 Hz, *C*H), 133.77 (s, *C*H), 148.25 (s, *C*N), 154.19 (d, J_{C-P} = 1.4 Hz, *C*N). ^{31}P NMR (162 MHz, $CDCl_3$): δ 36.1 (s). HRMS (FAB) *m*/*z*: calcd for $C_{24}H_{21}N_2OP$, 384.1392; found, 384.1392 [M^+]. Anal. Calcd for $C_{24}H_{21}N_2OP$: C, 74.99; H, 5.51; N, 7.29. Found: C, 74.75; H, 5.60; N, 7.15.

Synthesis of 3 (another method). To a DMA solution (15 mL) of **1** (1.00 g, 3.24 mmol) were added $PdCl_2$ (10 mg, 56 μmol), diphenylphosphine (0.62 mL, 3.6 mmol), and AcONa (0.39 g, 0.50 mmol). After the solution was stirred at 130 °C for 12 h, the reaction mixture was washed with water and extracted with $CHCl_3$. Evaporation of the solvent gave a crude oil. Similar purification of the crude oil gave **3** (0.94 g, 76%).

Synthesis of Diphenyl[2-(1-phenylhydrazino)phenyl]phosphine sulfide (4). Similarly, the reaction of **2**, which was prepared from **1** (0.50 g, 1.62 mmol), with sulfur (0.14 g, 4.38 mmol as S) in toluene (10 mL) at room temperature for 5 h gave a colorless solid of **4** (0.47 g, 72%). Mp: 176−178 °C. ^1H NMR (500 MHz, $CDCl_3$): δ 5.55 (brs, 1H), 6.50 (d, $^3J_{H-H}$ = 8.0 Hz, 2H), 6.64 (ddd, $^3J_{H-P}$ = 14.0 Hz, $^3J_{H-H}$ = 7.5 Hz, $^4J_{H-H}$ = 1.5 Hz, 1H), 6.67 (td, $^3J_{H-H}$ = 7.5 Hz, J_{H-P} = 2.0 Hz, 1H), 6.74 (t, $^3J_{H-H}$ = 7.5 Hz, 1H), 7.06 (t, $^3J_{H-H}$ = 8.0 Hz, 2H), 7.21 (dd, $^3J_{H-H}$ = 7.5 Hz, J_{H-P} = 6.0 Hz, 1H), 7.35 (td, $^3J_{H-H}$ = 7.5 Hz, $^4J_{H-H}$ = 1.5 Hz, 1H), 7.48 (td, $^3J_{H-H}$ = 7.5 Hz, $^4J_{H-P}$ = 3.0 Hz, 4H), 7.56 (td, $^3J_{H-H}$ = 7.5 Hz, $^5J_{H-P}$ = 2.0 Hz, 2H), 7.76 (ddd, $^3J_{H-P}$ = 13.5 Hz, $^3J_{H-H}$ = 7.5 Hz, $^4J_{H-H}$ = 1.5 Hz, 4H), 8.25 (brs, 1H). $^{13}C\{^1H\}$ NMR (126 MHz, $CDCl_3$): δ 112.35 (s, *C*H), 112.51 (d, J_{C-P} = 7.3 Hz, *C*H), 112.57 (d, $^1J_{C-P}$ = 86.3 Hz, *C*P), 118.05 (d, J_{C-P} = 12.4 Hz, *C*H), 119.78 (s, *C*H), 128.69 (d, $^3J_{C-P}$ = 12.7 Hz, *C*H), 129.13 (s, *C*H), 131.29 (d, $^1J_{C-P}$ = 85.9 Hz, *C*P), 131.90 (s, *C*H), 132.48 (d, J_{C-P} = 10.8 Hz, *C*H), 132.70 (d, J_{C-P} = 8.8 Hz, *C*H), 133.57 (s, *C*H), 147.41 (s, *C*N), 151.18 (s, *C*N). ^{31}P NMR (162 MHz, $CDCl_3$) δ 39.4 (s). Anal. Calcd for $C_{24}H_{21}N_2PS$: C, 71.98; H, 5.29; N, 7.00. Found: C, 71.82; H, 5.36; N, 6.83.

Synthesis of Diphenyl[2-(1-phenylhydrazino)phenyl]phosphine selenide (5). Similarly, the reaction of **2**, which was prepared from **1** (0.50 g, 1.62 mmol), with elemental selenium (0.25 g, 0.32 mmol) in toluene (10 mL) at room temperature for 12 h gave a colorless solid of **5** (0.55 g, 75%). Mp: 166−167 °C. ^1H NMR (500 MHz, $CDCl_3$): δ 5.57 (brs, 1H), 6.53 (m, $^3J_{H-H}$ = 8.0 Hz, 2H), 6.63 (dd, $^3J_{H-P}$ = 11.8 Hz, $^3J_{H-H}$ = 7.5 Hz, 1H), 6.67−6.70 (m, 1H), 6.76 (t, $^3J_{H-H}$ = 7.5 Hz, 1H), 7.08 (t, $^3J_{H-H}$ = 8.0 Hz, 2H), 7.21−7.25 (m, 1H), 7.31 (t, $^3J_{H-H}$ = 7.5 Hz, 1H), 7.48 (td, $^3J_{H-H}$ = 7.5 Hz, J_{H-P} = 3.0 Hz, 4H), 7.55 (td, $^3J_{H-H}$ = 7.5 Hz, $^3J_{H-P}$ = 2.0 Hz, 2H), 7.78 (ddd, $^3J_{H-P}$ = 13.5 Hz, $^3J_{H-H}$ = 7.5 Hz, $^4J_{H-H}$ = 1.5 Hz, 4H), 8.26 (brs, 1H). $^{13}C\{^1H\}$ NMR (126 MHz, $CDCl_3$): δ 111.13 (d, $^1J_{C-P}$ = 74.5 Hz, *C*P), 112.37 (s, *C*H), 112.68 (d, J_{C-P} = 7.5 Hz, *C*H), 118.16 (d, J_{C-P} = 12.1 Hz, *C*H), 119.79 (s, *C*H), 128.71 (d, J_{C-P} = 12.5 Hz, *C*H), 129.30 (d, $^1J_{C-P}$ = 77.6 Hz, *C*P), 129.76 (s, *C*H), 131.96 (d, J_{C-P} = 2.8 Hz, *C*H), 132.48 (d, J_{C-P} = 8.4 Hz, *C*H), 132.50 (d, J_{C-P} = 11.1 Hz, *C*H), 133.63 (s, *C*H), 147.94 (s, *C*N), 151.85 (d, J_{C-P} = 3.5 Hz, *C*N). ^{31}P NMR (162 MHz, $CDCl_3$): δ 26.4 (s, $^1J_{P-Se}$ = 683.2 Hz). ^{77}Se NMR (95 MHz, $CDCl_3$): δ = −260.2 (d, $^1J_{Se-P}$ = 683.2 Hz). HRMS (FAB) *m*/*z*: calcd for $C_{24}H_{21}N_2P^{80}Se$, 448.0608; found, 448.0588 [M^+].

Typical Procedure for the Oxidation of Diphenyl[2-(1-phenylhydrazino)phenyl]phosphine Chalcogenides 3−5. To an EtOH solution (3 mL) of **3** (7 mg, 18 μmol) was added bromine (5 μL, 0.1 mmol), and the reaction solution was stirred at room temperature for 30 min. After the solvent was evaporated, quantitative formation of (*E*)-**7** was confirmed by ^1H and ^{31}P NMR spectra of the crude material. Oxidation reactions of **3**−**5** with pyridinium tribromide, *tert*-butyl hypochlorite, and 30% H_2O_2(aq) were similarly carried out. The results are summarized in Table 3.

Spectral and Analytical Data of (*E*)-7−(*E*)-9. (*E*)-7. Red solid ($CHCl_3$); mp: 159−160 °C. ^1H NMR (500 MHz, $CDCl_3$): δ 7.21 (d, $^3J_{H-H}$ = 7.5 Hz, 2H), 7.29 (t, $^3J_{H-H}$ = 7.5 Hz, 2H), 7.33−7.37 (m, 6H), 7.43 (td, $^3J_{H-H}$ = 7.5 Hz, $^4J_{H-H}$ = 1.5 Hz, 1H), 7.58 (t, $^3J_{H-H}$ = 7.5 Hz, 1H), 7.67 (t, $^3J_{H-H}$ = 7.5 Hz, 1H), 7.71−7.81 (m, 5H), 8.09 (ddd, $^3J_{H-P}$ = 12.0 Hz, $^3J_{H-H}$ = 7.5 Hz, $^4J_{H-H}$ = 1.5 Hz, 1H). $^{13}C\{^1H\}$ NMR (126 MHz, $CDCl_3$): δ 115.42 (d, J_{C-P} = 7.2 Hz, *C*H), 123.38 (s, *C*H), 128.26 (d, J_{C-P} = 13.0 Hz, *C*H), 128.76 (s, *C*H), 130.76 (d, J_{C-P} = 12.0 Hz, *C*H), 131.38 (s, *C*H), 131.38 (d, J_{C-P} = 7.4 Hz, *C*H), 131.70 (d, J_{C-P} = 10.8 Hz, *C*H), 132.34 (d, $^1J_{C-P}$ = 98.5 Hz, *C*P), 133.17 (d, J_{C-P} = 2.6 Hz, *C*H), 133.83 (d, $^1J_{C-P}$ = 108.2 Hz, *C*P), 134.54 (d, J_{C-P} = 10.0 Hz, *C*H), 152.24 (s, *C*N), 152.64 (d, J_{C-P} = 1.2 Hz, *C*N). ^{31}P NMR (162 MHz, $CDCl_3$): δ 28.0 (s). UV−vis ($CHCl_3$) λ_{max} (log ϵ): 327 (4.23), 458 nm (2.95). Anal. Calcd for $C_{24}H_{19}N_2OP$: C, 75.38; H, 5.01; N, 7.33. Found: C, 75.14; H, 5.01; N, 7.07.

(*E*)-8. Red solid ($CHCl_3$); mp: 133−135 °C. ^1H NMR (500 MHz, $CDCl_3$): δ 7.28−7.30 (m, 4H), 7.33−7.42 (m, 7H), 7.50 (t, $^3J_{H-H}$ = 7.5 Hz, 1H), 7.63 (t, $^3J_{H-H}$ = 7.5 Hz, 1H), 7.76 (dd, $^3J_{H-H}$ = 7.5 Hz, J_{H-P} = 4.8 Hz, 1H), 7.80 (dd, $^3J_{H-H}$ = 7.5 Hz, $^4J_{H-H}$ = 1.5 Hz, 1H), 7.87 (ddd, $^3J_{H-P}$ = 15.0 Hz, $^3J_{H-H}$ = 7.5 Hz, $^4J_{H-H}$ = 1.5 Hz, 4H). $^{13}C\{^1H\}$ NMR (126 MHz, $CDCl_3$): δ 115.76 (d, J_{C-P} = 7.2 Hz, *C*H), 123.62 (s, *C*H), 128.25 (d, J_{C-P} = 13.2 Hz, *C*H), 128.74 (s, *C*H), 130.58 (d, J_{C-P} = 12.0 Hz, *C*H), 131.00 (d, J_{C-P} = 2.6 Hz, *C*H), 131.40 (s, *C*H), 131.84 (d, $^1J_{C-P}$ = 81.8 Hz, *C*P), 131.89 (d, J_{C-P} = 10.8 Hz, *C*H), 132.93 (d, J_{C-P} = 2.4 Hz, *C*H), 133.82 (d, $^1J_{C-P}$ = 87.7 Hz, *C*P), 134.39 (d, J_{C-P} = 10.0 Hz, *C*H), 152.16 (d, J_{C-P} = 1.2 Hz, *C*N), 152.27 (s, *C*N). ^{31}P NMR (162 MHz, $CDCl_3$): δ 42.8 (s). UV−vis ($CHCl_3$) λ_{max} (log ϵ): 328 (4.20), 465 nm (2.95). Anal. Calcd for $C_{24}H_{19}N_2PS$: C, 72.34; H, 4.81; C, 7.03. Found: C, 72.09; H, 4.93; N, 6.73.

(*E*)-9. Red solid ($CHCl_3$); mp: 130−131 °C. ^1H NMR (500 MHz, $CDCl_3$): δ 7.26−7.30 (m, 4H), 7.32−7.38 (m, 7H), 7.48 (t, $^3J_{H-H}$ = 7.5 Hz, 1H), 7.63 (t, $^3J_{H-H}$ = 7.5 Hz, 1H), 7.69 (dd, $^3J_{H-P}$ = 15.0 Hz, $^3J_{H-H}$ = 7.5 Hz, 1H), 7.76 (dd, $^3J_{H-H}$ = 7.5 Hz, J_{H-P} = 4.6 Hz, 1H), 7.88 (dd, $^3J_{H-P}$ = 14.0 Hz, $^3J_{H-H}$ = 7.5 Hz, 4H). $^{13}C\{^1H\}$ NMR (126 MHz, $CDCl_3$): δ 115.90 (d, J_{C-P} = 6.8 Hz, *C*H), 123.76 (s, *C*H), 128.29 (d, J_{C-P} = 12.5 Hz, *C*H), 128.78 (s, *C*H), 130.59 (d, J_{C-P} = 12.6 Hz, *C*H), 131.09 (d, J_{C-P} = 2.9 Hz, *C*H), 131.43 (s, *C*H), 131.61 (d, $^1J_{C-P}$ = 73.6 Hz, *C*P), 132.42 (d, $^1J_{C-P}$ = 79.4 Hz, *C*P), 132.47 (d, J_{C-P} = 10.9 Hz, *C*H), 133.01 (d, J_{C-P} = 2.5 Hz, *C*H), 134.69 (d, J_{C-P} = 10.3 Hz, *C*H), 152.04 (d, J_{C-P} = 2.8 Hz, *C*N), 152.32 (s, *C*N). ^{31}P NMR (162 MHz, $CDCl_3$): δ 33.3 (s, $^1J_{P-Se}$ = 732.4 Hz). ^{77}Se NMR (95 MHz, $CDCl_3$) δ −179.2 (d, $^1J_{Se-P}$ = 732.4 Hz). UV−vis ($CHCl_3$) λ_{max} (log ϵ): 325 (4.23), 465 nm (2.95). Anal. Calcd for $C_{24}H_{19}N_2PSe$: C, 64.73; H, 4.30; N, 6.29. Found: C, 64.51; H, 4.55; N, 6.19.

Synthesis of (*E*)-Hydroxydiphenyl[2-(phenylazo)phenyl]phosphonium Triflate ((*E*)-10). To a benzene solution (5 mL) of (*E*)-**7** (100 mg, 0.262 mmol) was added TMSOTf (0.1 mL) at room temperature. After the solvent was evaporated, recrystallization of the residue from wet benzene gave a red solid of (*E*)-**10** (75 mg, 54%). ^1H NMR (500 MHz, C_6D_6): δ 6.86 (td, $^3J_{H-H}$ = 7.5 Hz, J_{H-P} = 3.5 Hz, 4H), 6.93 (dd, $^3J_{H-H}$ = 7.5 Hz, $^4J_{H-H}$ = 1.5 Hz, 2H), 6.96−7.00 (m, 3H), 7.04 (tdd, $^3J_{H-H}$ = 7.5 Hz, $^4J_{H-H}$ = 1.5 Hz, J_{H-P} = 1.0 Hz, 1H), 7.11 (tt, $^3J_{H-H}$ = 7.5 Hz, $^4J_{H-H}$ = 1.5 Hz, 1H), 7.22 (dd, $^3J_{H-H}$ = 7.5 Hz, $^4J_{H-H}$ = 1.5 Hz, 2H), 7.60 (ddd,

$^3J_{H-P}$ = 14.0 Hz, $^3J_{H-H}$ = 7.5 Hz, $^4J_{H-H}$ = 1.5 Hz, 4H), 7.67 (ddd, $^3J_{H-H}$ = 7.5 Hz, J_{H-P} = 5.0 Hz, $^4J_{H-H}$ = 1.5 Hz, 1H), 7.99 (ddd, $^3J_{H-P}$ = 13.5 Hz, $^3J_{H-H}$ = 7.5 Hz, $^4J_{H-H}$ = 1.5 Hz, 1H). $^{13}C\{^1H\}$ NMR (126 MHz, C_6D_6): δ 116.57 (d, J_{C-P} = 8.4 Hz, *C*H), 121.12 (q, $^1J_{C-F}$ = 320.9 Hz, *C*F$_3$), 123.68 (s, *C*H), 124.57 (d, $^1J_{C-P}$ = 108.2 Hz, *C*P), 126.02 (d, $^1J_{C-P}$ = 113.0 Hz, *C*P), 129.28 (d, J_{C-P} = 13.2 Hz, *C*H), 129.30 (s, *C*H), 131.97 (d, J_{C-P} = 12.0 Hz, *C*H), 132.39 (d, J_{C-P} = 10.8 Hz, *C*H), 132.57 (s, *C*H), 133.93 (s, *C*H), 135.20 (d, J_{C-P} = 8.4 Hz, *C*H), 135.87 (s, *C*H), 152.25 (s, *C*N), 152.96 (d, J_{C-P} = 4.8 Hz, *C*N). ^{19}F NMR (376 MHz, C_6D_6): δ −78.42 (s). ^{31}P NMR (162 MHz, C_6D_6): δ 48.5 (s). UV−vis ($CHCl_3$) λ_{max} (log ϵ): 332 (4.18), 460 nm (2.95).

Synthesis of (*E*)-Diphenyl[4-(phenylazo)phenyl]phosphine ((*E*)-14). To an Et_2O solution (30 mL) of 4-iodoazobenzene (**13**) (100 mg, 0.324 mmol) at −105 °C was rapidly added *n*-BuLi (1.6 M in hexane, 0.21 mL, 0.34 mmol). After the reaction solution was stirred further at −105 °C for 5 min, diphenylthiophosphinoyl chloride (68 μL, 0.36 mmol) was added at −105 °C and stirred at room temperature for 3 h. After the addition of water, extraction with $CHCl_3$ and evaporation of the solvent gave a crude solid. The crude solid was separated by silica gel chromatography (eluent: $CHCl_3$), and recrystallization from hexane gave an orange solid of (*E*)-**14** (113 mg, 90%). Mp: 98−100 °C. ^1H NMR (500 MHz, $CDCl_3$): δ 7.29−7.37 (m, 10H), 7.42 (dd, $^3J_{H-P}$ = 8.5 Hz, $^3J_{H-H}$ = 7.5 Hz, 2H), 7.47−7.53 (m, 3H), 7.85 (dd, $^3J_{H-H}$ = 7.5 Hz, $^4J_{H-H}$ = 1.5 Hz, 2H), 7.90 (dd, $^3J_{H-H}$ = 7.5 Hz, $^4J_{H-H}$ = 1.5 Hz, 2H). $^{13}C\{^1H\}$ NMR (126 MHz, $CDCl_3$): δ 122.72 (d, J_{C-P} = 6.8 Hz, *C*H), 122.95 (s, *C*H), 128.69 (d, J_{C-P} = 7.2 Hz, *C*H), 129.07 (s, *C*H), 129.14 (s, *C*H), 131.21 (s, *C*H), 133.94 (d, J_{C-P} = 19.8 Hz, *C*H), 134.38 (d, J_{C-P} = 2.6 Hz, *C*H), 136.61 (d, $^1J_{C-P}$ = 10.7 Hz, *C*P), 141.20 (d, $^1J_{C-P}$ = 13.1 Hz, *C*P), 152.58 (s, *C*N), 152.65 (s, *C*N). ^{31}P NMR (162 MHz, $CDCl_3$): δ −4.4 (s). UV−vis ($CHCl_3$) λ_{max} (log ϵ): 340 nm (4.25). Anal. Calcd for $C_{24}H_{19}N_2P$: C, 78.67; H, 5.23; N, 7.65. Found: C, 78.50; H, 5.30; N, 7.49.

Spectral and Analytical Data of (*E*)-15−(*E*)-17. (*E*)-15. Mp: 169−170 °C. ^1H NMR (500 MHz, $CDCl_3$): δ 7.46−7.58 (m, 9H), 7.70 (dd, $^3J_{H-P}$ = 12.5 Hz, $^3J_{H-H}$ = 8.0 Hz, 4H), 7.83 (dd, $^3J_{H-P}$ = 11.5 Hz, $^3J_{H-H}$ = 8.0 Hz, 2H), 7.91−7.97 (m, 4H). $^{13}C\{^1H\}$ NMR (126 MHz, $CDCl_3$): δ 122.62 (d, J_{C-P} = 12.6 Hz, *C*H), 123.13 (s, *C*H), 128.62 (d, J_{C-P} = 12.5 Hz, *C*H), 129.17 (s, *C*H), 131.77 (s, *C*H), 132.06 (d, J_{C-P} = 10.0 Hz, *C*H), 132.09 (d, $^1J_{C-P}$ = 105.2 Hz, *C*P), 132.16 (d, J_{C-P} = 1.8 Hz, *C*H), 133.10 (d, J_{C-P} = 7.9 Hz, *C*H), 134.83 (d, J_{C-P} = 103.3 Hz, *C*P), 152.93 (s, *C*N), 154.47 (s, *C*N). ^{31}P NMR (162 MHz, $CDCl_3$): δ 29.1 (s). UV−vis ($CHCl_3$) λ_{max} (log ϵ): 324 (4.23), 440 nm (2.85). Anal. Calcd for $C_{24}H_{19}N_2OP$: C, 75.38; H, 5.01; N, 7.33. Found: C, 75.29; H, 5.09; N, 7.18.

(*E*)-16. Mp: 136−138 °C. ^1H NMR (500 MHz, $CDCl_3$): δ 7.43−7.49 (m, 4H), 7.50−7.55 (m, 5H), 7.75 (dd, $^3J_{H-P}$ = 13.5 Hz, $^3J_{H-H}$ = 8.0 Hz, 4H), 7.86 (dd, $^3J_{H-P}$ = 12.5 Hz, $^3J_{H-H}$ = 8.0 Hz, 2H), 7.91−7.95 (m, 4H). $^{13}C\{^1H\}$ NMR (126 MHz, $CDCl_3$): δ 122.52 (d, J_{C-P} = 13.4 Hz, *C*H), 123.07 (s, *C*H), 128.56 (d, J_{C-P} = 12.5 Hz, *C*H), 129.09 (s, *C*H), 131.62 (s, *C*H), 131.63 (s, *C*H), 132.16 (d, J_{C-P} = 10.8 Hz, *C*H), 132.64 (d, $^1J_{C-P}$ = 84.1 Hz, *C*P), 133.17 (d, J_{C-P} = 11.6 Hz, *C*H), 135.24 (d, $^1J_{C-P}$ = 83.5 Hz, *C*P), 152.40 (s, *C*N), 154.08 (d, J_{C-P} = 3.3 Hz, *C*N). ^{31}P NMR (162 MHz, $CDCl_3$): δ 43.5 (s). UV−vis ($CHCl_3$) λ_{max} (log ϵ): 324 (4.23), 440 nm (2.85). Anal. Calcd for $C_{24}H_{19}N_2PS$: C, 72.34; H, 4.81; N, 7.03. Found: C, 72.26; H, 4.94; N, 6.85.

(*E*)-17. ^1H NMR (500 MHz, $CDCl_3$): δ 7.46 (dd, $^3J_{H-H}$ = 8.0 Hz, J_{H-P} = 2.5 Hz, 4H), 7.50−7.54 (m, 5H), 7.76 (dd, $^3J_{H-P}$ = 13.5 Hz, $^3J_{H-H}$ = 8.0 Hz, 4H), 7.86 (dd, $^3J_{H-P}$ = 13.0 Hz, $^3J_{H-H}$ = 8.0 Hz, 2H), 7.91−7.95 (m, 4H). $^{13}C\{^1H\}$ NMR (126 MHz, $CDCl_3$): δ 122.62 (d, J_{C-P} = 12.6 Hz, *C*H), 123.18 (s, *C*H), 128.69 (d, J_{C-P} = 12.6 Hz, *C*H), 129.21 (s, *C*H), 131.41 (d, $^1J_{C-P}$ = 78.2 Hz, *C*P), 131.83 (s, *C*H), 131.84 (s, *C*H), 132.65 (d, J_{C-P} = 11.0 Hz, *C*H), 133.63 (d, J_{C-P} = 11.6 Hz, *C*H), 134.11 (d, $^1J_{C-P}$ = 76.1 Hz, *C*P), 152.44 (s, *C*N), 154.11 (d, J_{C-P} = 3.5 Hz, *C*N). ^{31}P NMR (162 MHz, $CDCl_3$): δ 35.5 (s, $^1J_{P-Se}$ = 736.0 Hz). ^{77}Se NMR (95 MHz, $CDCl_3$): δ −263.4 (d, $^1J_{Se-P}$ = 736.0 Hz). UV−vis ($CHCl_3$) λ_{max} (log ϵ): 324 (4.23), 440 nm (2.85). HRMS (FAB) *m*/*z*: calcd for $C_{24}H_{19}N_2P^{80}Se$, 446.0451; found, 446.0443 [M^+].

Typical Procedure of Photoisomerization of (*E*)-7 and (*E*)-15−(*E*)-17. A $CDCl_3$ solution (0.5 mL) of (*E*)-**7** (1.3 mg, 3.4 μmol) was irradiated with a high-pressure mercury lamp through a color glass filter (λ = 360 nm) for 1 h in the dark room. In the ^1H NMR spectrum, the ratio of (*E*)-**7**:(*Z*)-**7** was determined to be 90:10. Irradiation (λ = 445 nm) of (*Z*)-**7** changed the ratio of (*E*)-**7**:(*Z*)-**7** to 81:19. Results of photoisomerization are summarized in Schemes 6 and 7.

Spectral and Analytical Data of (*Z*)-7 and (*Z*)-15−(*Z*)-(17). (*Z*)-7. ^1H NMR (500 MHz, $CDCl_3$): δ 6.06 (dd, $^3J_{H-H}$ = 7.5 Hz, J_{H-P} = 5.0 Hz, 1H), 6.65 (d, $^3J_{H-H}$ = 7.5 Hz, 2H), 7.08−7.24 (m, 5H), 7.45−7.53 (m, 7H), 7.88 (dd, $^3J_{H-P}$ = 13.0 Hz, $^3J_{H-H}$ = 8.0 Hz, 4H). ^{31}P NMR (162 MHz, $CDCl_3$): δ 28.1 (s).

(*Z*)-15. ^1H NMR (500 MHz, $CDCl_3$): δ 6.83 (d, $^3J_{H-H}$ = 8.0 Hz, 2H), 6.88 (dd, $^3J_{H-H}$ = 8.0 Hz, $^4J_{H-H}$ = 1.5 Hz, 2H), 7.18 (t, $^3J_{H-H}$ = 8.0 Hz, 1H), 7.42−7.48 (m, 5H), 7.57−7.62 (m, 9H). ^{31}P NMR (162 MHz, $CDCl_3$): δ 29.3 (s).

(*Z*)-16. ^1H NMR (500 MHz, $CDCl_3$): δ 6.84 (d, $^3J_{H-H}$ = 8.0 Hz, 2H), 6.88 (dd, $^3J_{H-H}$ = 8.0 Hz, $^4J_{H-H}$ = 1.5 Hz, 2H), 7.18 (t, $^3J_{H-H}$ = 8.0 Hz, 1H), 7.24−7.28 (m, 2H), 7.41−7.45 (m, 4H), 7.51 (t, $^3J_{H-H}$ = 8.0 Hz, 2H), 7.58−7.65 (m, 6H). ^{31}P NMR (162 MHz, $CDCl_3$): δ 43.3 (s).

(*Z*)-17. ^1H NMR (500 MHz, $CDCl_3$): δ 6.84 (d, $^3J_{H-H}$ = 8.0 Hz, 2H), 6.87 (dd, $^3J_{H-H}$ = 8.0 Hz, 2H), 7.17 (t, $^3J_{H-H}$ = 8.0 Hz, 1H), 7.25−7.28 (m, 2H), 7.40−7.50 (m, 4H), 7.58−7.64 (m, 8H). ^{31}P NMR (162 MHz, $CDCl_3$): δ 35.8 (s).

X-ray Crystallographic Analyses of 2−5 and (*E*)-7−(E)-10. Intensities of reflections were collected on a Rigaku Mercury CCD diffractometer with graphite-monochromated Mo−Kα radiation (λ = 0.71070 Å) using CrystalClear (Rigaku Corp.). The data were corrected for Lorentz polarization effects. The structure was solved by direct methods (SIR97) and expanded using Fourier techniques.[26] The non-hydrogen atoms were refined anisotropically and hydrogen atoms were refined isotropically with SHELX-97.[27] CCDC-292658 (**2**), CCDC-292659 (**3**), CCDC-292660 (**4**), CCDC-292661 (**5**), CCDC-292662 ((*E*)-**7**), CCDC-292663 ((*E*)-**8**), CCDC-292664 ((*E*)-**9**), and CCDC-292665 ((*E*)-**10**) contain the supplementary crystallographic data for this paper. These data can be obtained free of charge from the Cambridge Crystallographic Data Centre via www.ccdc.cam.uk/data-request/cif.

Acknowledgment. We thank Shin-etsu Chemical Co., Ltd., and Tosoh Finechem Corp. for gifts of TMSOTf and alkyllithiums, respectively. This work was partially supported by Grants-in-Aid from the 21st Century COE Program for Frontiers in Fundamental Chemistry and for Scientific

(26) Altomare, A.; Burla, M.; Camalli, M.; Cascarano, G.; Giacovazzo, C.; Guagliardi, A.; Moliterni, A.; Polidori, G.; Spagna, R. *J. Appl. Crystallogr.* **1999**, *32*, 115−119.

(27) Sheldrick, G. M. *SHELX-97*: *Program for the Solution and Refinement of Crystal Structures*; Universität Göttingen: Göttingen, Germany, 1997.

Research 14740395 (N.K.), 15105001 (T.K.), 16033215 (T.K.), and 1611512 (M.Y.) from the Ministry of Education, Culture, Sports, Science and Technology, Japan, as well as by the Japan Society for Promotion of Science and Dainippon Ink and Chemicals, Inc.

Supporting Information Available: Detailed synthetic procedure of (*E*)-**15**−(*E*)-**17** and ^{1}H NMR spectra of **7** and **15**−**17** before and after photoirradiation. This material is available free of charge via the Internet at http://pubs.acs.org.

IC0601790